nature cell biology

UNC-6 (netrin) orients the invasive membrane of the anchor cell in *C. elegans*

Joshua W. Ziel[1], Elliott J. Hagedorn[1], Anjon Audhya[2] and David R. Sherwood[1,3,4]

Despite their profound importance in the development of cancer, the extracellular cues that target cell invasion through basement membrane barriers remain poorly understood[1]. A central obstacle has been the difficulty of studying the interactions between invading cells and basement membranes *in vivo*[2,3]. Using the genetically and visually tractable model of *Caenorhabditis elegans* anchor cell (AC) invasion, we show that UNC-6 (netrin) signalling, a pathway not previously implicated in controlling cell invasion *in vivo*, is a key regulator of this process. Site of action studies reveal that before invasion, localized UNC-6 secretion directs its receptor, UNC-40, to the plasma membrane of the AC, in contact with the basement membrane. There, UNC-40 polarizes a specialized invasive membrane domain through the enrichment of actin regulators, F-actin and phosphatidylinositol 4,5-bisphosphate (PtdIns(4,5)P$_2$). Cell ablation experiments indicate that UNC-6 promotes the formation of invasive protrusions from the AC that break down the basement membrane in response to a subsequent vulval cue. Together, these results characterize an invasive membrane domain *in vivo*, and reveal a role for UNC-6 (netrin) in polarizing this domain towards its basement membrane target.

From its position in the developing uterus, the *C. elegans* anchor cell (AC) breaks through the juxtaposed gonadal and ventral epidermal basement membranes and inserts between the central primary-fated vulval precursor cells (1°-VPCs) to mediate a uterine–vulval connection (Fig. 1a, f)[4,5]. AC invasion is regulated by FOS-1A, the *C. elegans* orthologue of the Fos bZIP transcription factor. FOS-1A controls the expression of genes in the AC that mediate basement membrane breakdown[6–8]. Although required for invasion, FOS-1A is not sufficient to promote basement membrane removal. Breaching the basement membrane also depends on a signal from the 1°-VPCs that activates a FOS-1A-independent pathway that stimulates the extension of invasive processes from the basal membrane of the AC[5]. However, neither the molecular identity of the vulval cue nor the mechanisms that control the polarized invasive response are known.

To identify signalling pathways that promote invasive protrusions, we examined *C. elegans* strains with mutations in genes important for cellular motility (Supplementary Information, Table S1) and found that animals harbouring mutations in the guidance factor *unc-6* (netrin) or its receptor *unc-40* (DCC) showed the greatest defects in AC invasion. The netrin signalling pathway regulates numerous developmental events involving migrations through the basement membrane[9]; however, a direct role for netrin in regulating cell-invasive behaviour has not been demonstrated. Examination of animals at the mid to late L3 stage (P6.p 4-cell) revealed that the AC failed to invade in *unc-6(ev400)* and *unc-40(e271)* mutants (Fig. 1b; Supplementary Information, Table S2), and only partially completed a delayed invasion by the L4 stage (P6.p 8-cell; Supplementary Information, Table S2). Consistent with this receptor–ligand pair functioning together, *unc-40;unc-6* double-mutant animals had a similar invasion defect (Supplementary Information, Table S2). Inspection of *unc-6* and *unc-40* mutants before invasion indicated that in most cases, the AC was situated normally over the vulval cells (*n* = 104/119 and 154/175 animals, respectively), demonstrating a specific invasion defect rather than an indirect consequence of AC mispositioning[10].

To determine whether UNC-6 regulates the generation of invasive protrusions, we ablated all VPCs except the posterior-most P8.p cell in wild-type and *unc-6* mutant animals. The descendants of these isolated P8.p cells adopt the 1°-VPC fate (Fig. 1c, f), generate the stimulatory invasion cue, and then move towards the AC, providing an assay for the ability of the AC to extend invasive processes[5]. In contrast to wild-type animals, which directed invasive processes from all distances examined (Fig. 1c), ACs in *unc-6* mutants never extended invasive protrusions, even when bordered by 1°-VPCs (Fig. 1d, e). These experiments suggest that UNC-6 is either a component of the 1°-vulval signal or is required for the formation of invasive protrusions in response to this cue.

Previous work has indicated that UNC-6 is expressed in neurons of the ventral nerve cord (VNC) from the L1 stage to the adult stage, but not in the 1°-VPCs until the late L3 stage, after the AC breaches the basement membrane[11,12]. We confirmed these studies using a *unc-6* transcriptional reporter (Supplementary Information, Fig. S1)

[1]Department of Biology, Duke University, Box 90338, Durham, NC 27708 USA. [2]Department of Biomolecular Chemistry, University of Wisconsin-Madison, 1300 University Avenue, Madison, WI 53706, USA. [3]Molecular Cancer Biology Program, Duke University Medical Center, Durham, NC 27708 USA.
[4]Correspondence should be addressed to D.R.S. (e-mail: david.sherwood@duke.edu)
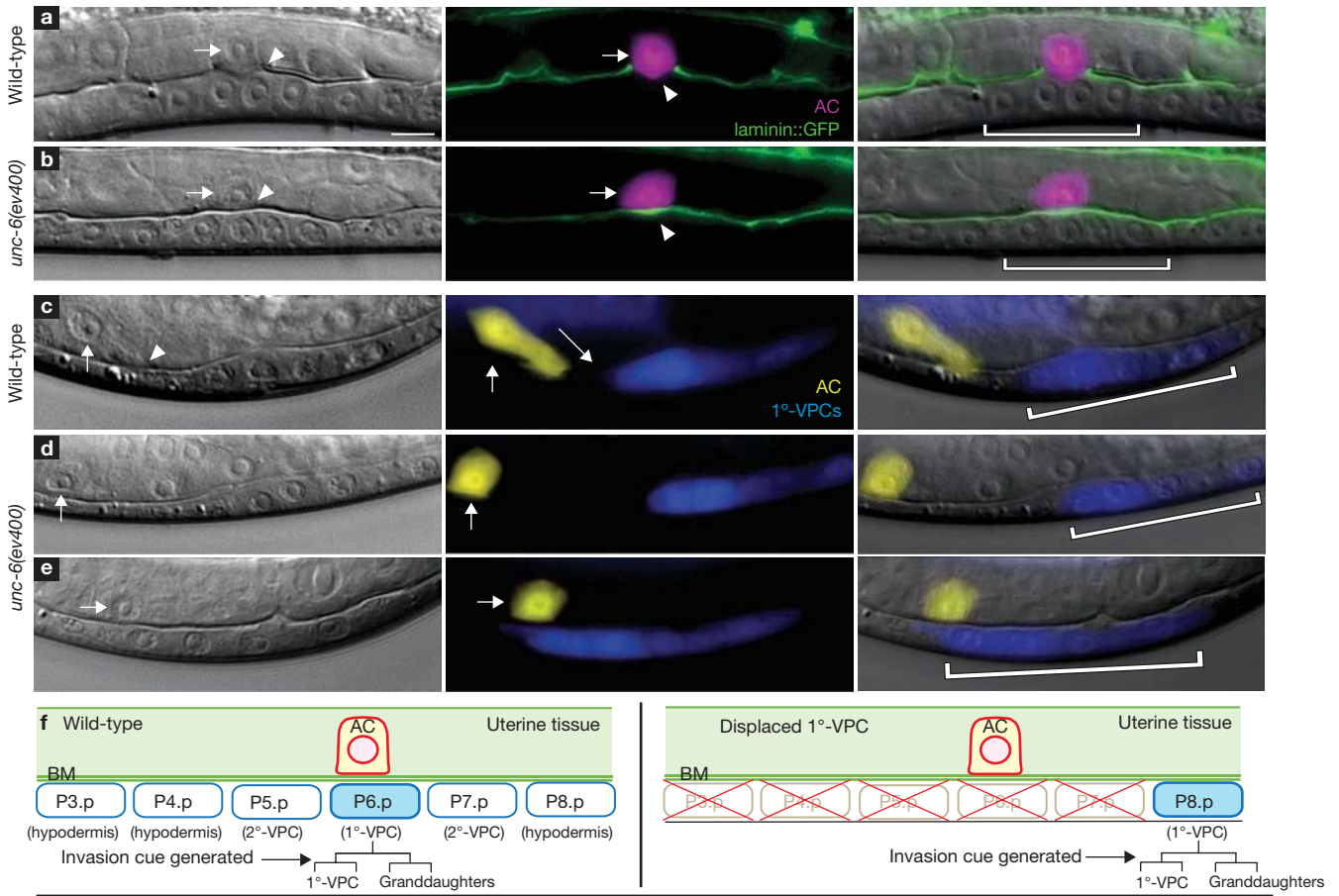
Figure 1 The AC fails to invade in *unc-6* mutants. (**a**–**e**) Nomarski (left), fluorescence microscopy (centre), and overlaid images (right) show that the wild-type AC (**a**; arrows; expressing *zmp-1*>mCherry in magenta) has crossed the basement membrane (arrowhead; interruption of phase-dense line on left and basement membrane component laminin, LAM-1::GFP in green) and contacted the central primary-fated P6.p granddaughters (P6.p 4-cell stage; 20/20 animals). In *unc-6* mutants (**b**), the basement membrane was intact under the AC in most animals (18/21 animals), and showed only small gaps in those that had partially invaded (3/21 animals, not shown). In wild-type animals the AC (expressing *cdh-3*>YFP in yellow, **c**) extended invasive processes toward isolated 1°-fated P8.p cell descendants (expressing *egl-17*>CFP in blue) in all cases examined (up to 25 μm away; 42/42 animals). In *unc-6* mutants, the AC failed to extend invasive processes toward 1°-fated P8.p cell descendants (**d**, **e**, 44/44 animals), even when they directly bordered the AC (**e**, 9/9 animals). Late L3 animals; anterior, left; ventral, down; bracket, 1°-VPCs. (**f**) Diagram showing the AC in wild-type animals at the early L3 stage (P6.p 1-cell stage, left) and after ablation of the VPCs P3.p through P7.p (right). Both diagrams show animals before division of the 1°-VPC (shown in blue). Future divisions of the 1°-VPC before and during invasion are shown below in brackets. The arrow points to the time that the 1°-vulval cue that stimulates invasion is generated. At this time the AC breaks through the underlying gonadal and ventral epidermal basement membranes (BM) and invades towards the 1°-VPCs. Scale bar, 5 μm for this and all other figures.

and a rescuing *Venus::unc-6* transgene. Notably, in addition to previously reported expression, low levels of full-length Venus::UNC-6 were observed in the basement membrane under the AC (Fig. 2a, b), probably originating from the VNC. Site of action studies revealed that VNC-specific expression of Venus::UNC-6[11] restored normal AC invasion in 90% of *unc-6* animals (Supplementary Information, Table S2). In contrast, Venus::UNC-6-driven expression in the 1°-VPCs[13] (mirroring the predicted expression of the vulval cue) did not rescue invasion (Supplementary Information, Table S2), suggesting that the timing of expression or processing of UNC-6 by the 1°-VPCs is not sufficient to stimulate invasion. Finally, 1°-VPC-specific RNAi-mediated knockdown of *unc-6* (*egl-17*>*mrfp::rde-1*; *rde-1(ne219)*) did not cause AC invasion defects (Supplementary Information, Table S2)[11]. These results suggest that UNC-6 is not the vulval cue, but rather a VNC-derived signal that promotes AC invasion.

To establish genetically whether UNC-6 functions as a separate non-vulval cue, we created vulvaless animals (see Methods) carrying the *unc-6* mutation. We have previously shown that approximately 20% of ACs invade in vulvaless animals (created by laser ablation or loss of vulval induction; Fig. 2c; Supplementary Information, Table S2)[5]. If *unc-6* encodes the vulval cue or regulates its secretion, loss of *unc-6* would not enhance the invasion defect in vulvaless animals. Alternatively, if UNC-6 is a distinct signal, its loss should augment the invasion defect of vulvaless animals. Supporting this second possibility, ACs in vulvaless animals harbouring the *unc-6* mutation had a dramatically more severe invasion defect: ACs never invaded and most detached from the basement membrane (Fig. 2d; Supplementary Information, Table S2). Furthermore, removal of the vulval cells had no effect on UNC-6 expression or localization (Supplementary Information, Fig. S2). We conclude that UNC-6 is a separate VNC-derived signal that regulates AC invasion.
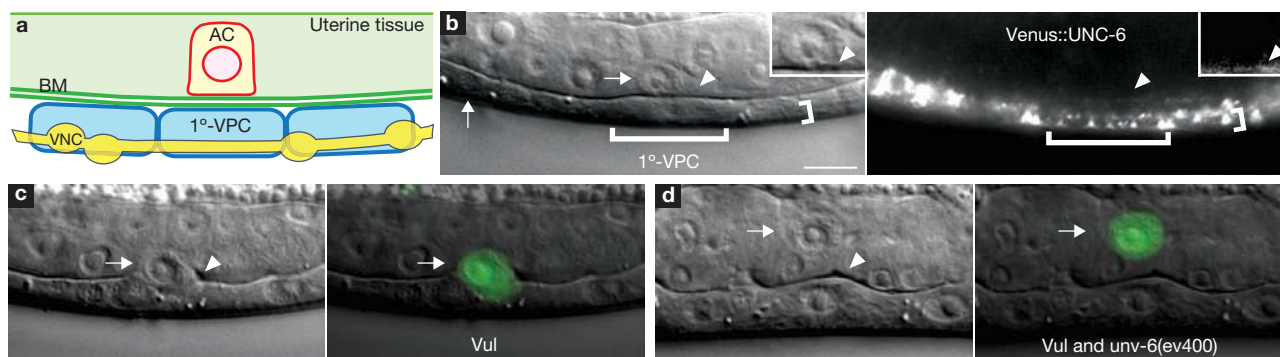
Figure 2 UNC-6 is a distinct VNC-derived, pro-invasive cue. (**a**) A diagram of the left side of the animal showing the relationship between the AC, basement membrane (BM), 1°-VPC and the neighbouring ventral nerve cord (VNC), with associated cell bodies (yellow ovals). (**b**) Nomarski (left) and fluorescence (right) images of an animal expressing Venus::UNC-6, viewed at the focal plane between the 1°-VPC (large bracket) and the VNC. Venus::UNC-6 accumulated in the VNC (small bracket. The vertical arrow points to VNC cell body where accumulation was strongest), and low levels were found in the basement membrane underlying the AC (arrowheads). The arrow points to the AC. Insets show an enlarged image of the AC with Venus::UNC-6 localization ventrally in the basement membrane (arrowheads). (**c**) In approximately 20% of vulvaless animals the AC invades into the underlying epidermis (both in *lin-3* loss of function mutants or when removed by laser ablation; Supplementary Information, Table S2). A Nomarski image (left) and a *cdh-3*>GFP overlay (right) show an AC in a vulvaless animal (arrow) that has broken through the underlying basement membrane and invaded (arrowhead). (**d**) In vulvaless animals carrying the *unc-6* mutation, the AC never invaded (70/70 animals) and usually detached from the basement membrane at the early L4 stage (arrowhead; 65/70 animals; Supplementary Information, Table S2).

Expression of the UNC-6 receptor, UNC-40::GFP, driven by an AC-specific *cis*-regulatory element (Supplementary Information, Fig. S3)[8] restored normal invasion in 96% of *unc-40* mutant animals (Supplementary Information, Table S2), demonstrating that UNC-6 signals directly to the AC to promote invasion. Beginning 5–6 h before invasion, UNC-40::GFP was found within intracellular vesicles and polarized along the invasive plasma membrane of the AC (Fig. 3a–c). UNC-40::GFP localization was normal in vulvaless animals (Fig. 3f), however, loss of UNC-6 resulted in the mislocalization of UNC-40::GFP along lateral and apical membranes (Fig. 3d, f; Supplementary Information, Table S3). To determine whether the ventral presentation of UNC-6 is required to target AC invasion and UNC-40::GFP localization, we drove ubiquitous expression of a haemag-glutinin (HA)-tagged UNC-6 protein (UNC-6::HA) under the control of the heat-shock promoter *hsp-16-2* before invasion (*hs>unc-6::HA*)[14]. Non-localized expression of UNC-6::HA led to disruptions in AC invasion at all time-points examined. The perturbations peaked 4 h after heat-shock (Supplementary Information, Table S2), and resulted in mislocalization of UNC-40::GFP (Fig. 3e, f; Supplementary Information, Table S3)**.** Thus, localization of UNC-40 to the invasive cell membrane is a specific targeting event mediated by UNC-6, and is required to promote invasion.

In neurons, signalling downstream of UNC-40 is mediated in part by the actin regulators UNC-34 (Ena/VASP) and the Rac GTPase, CED-10 (ref. 15). Importantly, *unc-34* mutants had perturbations in AC invasion*,* as did animals carrying mutations in both *ced-10* and *mig-2,* a Rac homologue that often functions redundantly with *ced-10* (ref. 16) (Supplementary Information, Table S2), indicating that a similar downstream network acts within the AC. To probe the relationships between these genes, the actin cytoskeleton and *unc-6*, we examined functional translational fusions of GFP to MIG-2 and CED-10, as well as AC-specific expression of GFP-tagged UNC-34 and the filamen-tous actin-binding domain of the *moesin* gene (mCherry::moeABD)[17]. MIG-2, F-actin, CED-10 and UNC-34 were all tightly localized to the basal invasive membrane of the AC both before and during AC invasion (Fig. 4a, d; Supplementary Information, Fig. S4; data not shown). This polarization was unique to the AC, as CED-10::GFP and pan-uterine

mCherry::moeABD expression revealed that F-actin and CED-10 were not basally enriched in neighbouring uterine cells (Supplementary Information, Fig. S4; data not shown). Examination of MIG-2, F-actin and UNC-34 indicated that, like UNC-40, their polarized localization was dependent on UNC-6 (Fig. 4b, e, j, k; data not shown), but not on the 1°-vulval cue (Fig. 4c, f, j, k; data not shown). In contrast, PAR-3::GFP, which localizes to apical and lateral membranes in wild-type ACs and AJM-1::GFP, which marks nascent apical spot junctions, were normal in *unc-6* mutants (Supplementary Information, Fig. S5). Thus, UNC-6 has a specific role in orienting downstream effectors to a specialized invasive cell membrane, but not in establishing the overall polarity of the AC.

Recently, the phospholipid PtdIns(4,5)P$_2$ has been implicated in linking the cortical actin cytoskeleton and Rac proteins to the inner plasma mem-brane leaflet[18,19]. Strikingly, PtdIns(4,5)P$_2$ (visualized with the PH domain from phospholipase Cδ (PLCδ) fused to mCherry[20]) was concentrated specifically at the basal invasive cell membrane of the AC (Fig. 4g, l), but was not polarized to the basal region of neighbouring uterine cells (Supplementary Information, Fig. S6). In the absence of the 1°-vulval cue, PtdIns(4,5)P$_2$ was polarized (Fig. 4i, l); however, in *unc-6* mutants, PtdIns(4,5)P$_2$ was found throughout the AC plasma membrane (Fig. 4h, l). AC-specific sequestration of PtdIns(4,5)P$_2$ (*cdh-3*>mCherry::PLCδ^{PH})[18] caused delays in invasion and enhanced the invasion defects of both *unc-34* and *mig-2* mutants (Supplementary Information, Table S2). We suggest that UNC-6 also promotes invasion through regulation of PtdIns(4,5)P$_2$ localization at the invasive cell membrane.

We next examined the interaction of the FOS-1A pathway with UNC-6 signalling. AC behaviour in *fos-1a* mutants is distinct from *unc-6* animals. In *fos-1a(ar105)* mutants, the AC extends cellular processes that flatten at the basement membrane, revealing a specific inability to breach this barrier[8]. MIG-2::GFP, marking the invasive membrane, was localized nor-mally in *fos-1a* mutants, consistent with the ability of the AC to extend cellular processes (Supplementary Information, Fig. S7). Conversely, transcriptional reporters for FOS-1A and two of its downstream targets, ZMP-1, a matrix metalloproteinase, and hemicentin (HIM-4), a conserved extracellular matrix protein, were expressed normally in *unc-6* mutants
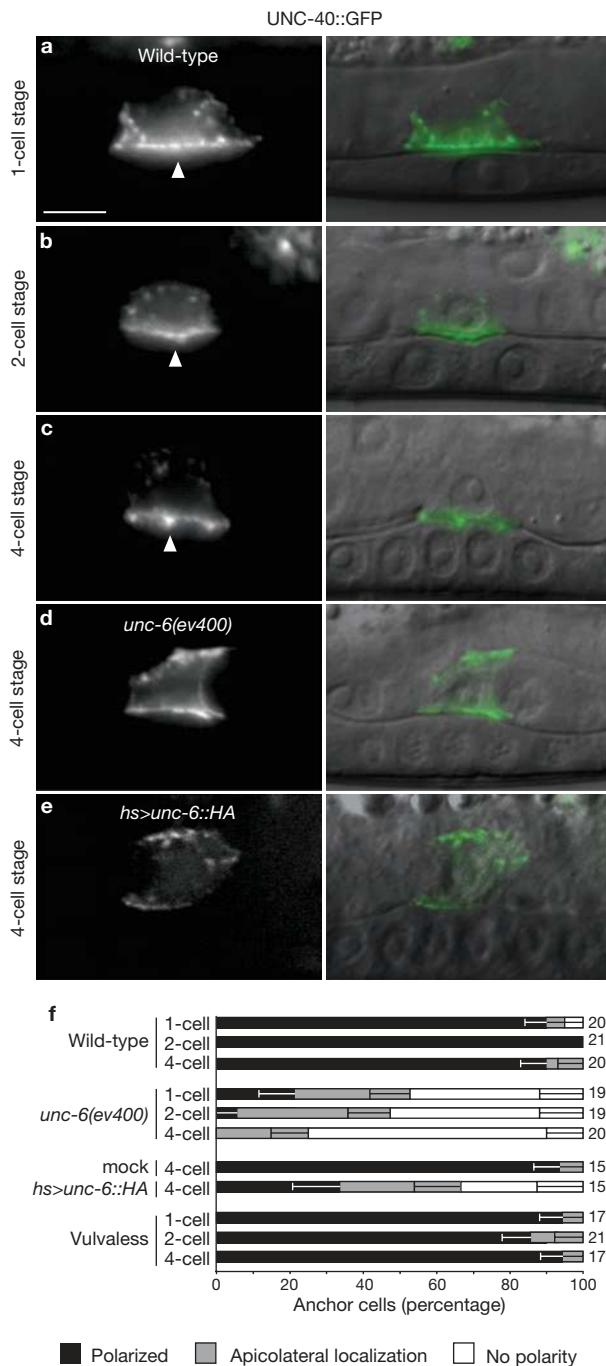
UNC-40::GFP

Figure 3 UNC-6 directs its receptor UNC-40 to the invasive cell membrane. (**a**–**e**) Fluorescence microscopy image (left), Nomarski overlay (right). UNC-40::GFP was present within intracellular vesicles and polarized to the invasive cell membrane of the AC (arrowheads) during the late L2 moult (P6.p 1-cell stage; 5–6 hours before invasion). UNC-40::GFP maintained this polarization until the time of invasion at the P6.p 4-cell stage (**a-c**). UNC-40::GFP polarization was perturbed in *unc-6* (**d**) mutants and in wild-type animals ubiquitously expressing UNC-6::HA induced by heat shock (**e**). (**f**) Compared with wild-type controls, UNC-40::GFP polarization in *unc-6* mutants, or following ubiquitous UNC-6::HA expression was significantly perturbed ($P < 7 \times 10^{-4}$ in all cases, Fisher's exact test in this and subsequent graphs). In contrast, neither vulvaless nor mock heat-shocked animals showed changes in UNC-40::GFP polarity, compared with wild-type ($P > 0.05$). The number of animals examined at each stage is listed to the right of the graph; error bars report s.e.m. of the proportion.

(Fig. 5a, b; data not shown). In addition, *fos-1* RNAi treatment of *unc-40* mutants resulted in an increased block in AC invasion (Supplementary Information, Table S2), indicating that FOS-1A has functions in AC invasion that are independent of the UNC-6 pathway.

Notably, however, the FOS-1A and UNC-6 pathways intersect at the invasive cell membrane. A putative *zmp-1*-null mutant has no invasion defect, and the ZMP-1 protein does not localize strongly to the invasive cell membrane, making its connection to FOS-1A activity and basement membrane breakdown unclear[8]. In contrast, null mutations in *him-4* cause a delay in AC invasion, and a functional HIM-4::GFP transgene is assembled specifically under the invasive cell membrane of the AC, where it aids in basement membrane removal during invasion (Fig. 5c)[8]. In *unc-6* mutants, there was a 65% reduction in HIM-4 deposited under the invasive cell membrane (Fig. 5c, d) and a threefold increase in HIM-4 accumulation along lateral and apical membranes of the AC, compared with wild-type controls (Supplementary Information, Movies S1, S2). Lack of HIM-4 is not sufficient to account for the severe block in AC invasion observed in *fos-1a* mutants, and another key downstream mediator(s) of FOS-1A remains to be identified[8]. Nevertheless, the failure of HIM-4 to be deposited normally indicates that the activities of the UNC-6 and FOS-1A pathways intersect at the invasive membrane, and that other targets of FOS-1A may similarly require UNC-6 for proper localization.

Taken together, our data demonstrate that UNC-6 generated from the VNC acts through its receptor UNC-40 in the AC to orient a specialized invasive membrane domain containing F-actin, actin regulators and PtdIns(4,5)P$_2$ towards the basement membrane. Site of action and genetics studies support a model where UNC-6 and the 1º-vulval cue act independently on the AC to promote invasion, a notion further strengthened by the distinct role for UNC-6 in polarizing the invasive membrane. The failure of the AC to extend robust invasive processes towards displaced 1º-vulval cells suggests that formation of the invasive membrane domain is required to respond to the vulval cue. UNC-6 is also necessary for normal HIM-4 deposition, a key FOS-1A target[8]. Thus, UNC-6 function is required for the integration of multiple pathways that converge at the invasive cell membrane to promote invasion (summarized in Fig. 5e).

Netrins are involved in a wide array of developmental events, including axon guidance, cell migration and synaptogenesis[9,10,21]. These cellular processes have recently been proposed to share an early polarization event mediated by UNC-6 signalling[21]. Our work supports this idea and further suggests that UNC-6 (netrin) may function generally to specify subcellular domains by localizing phosphoinositide species, such as PtdIns(4,5) P$_2$, F-actin and at least two of its major downstream effectors, UNC-34 (Enabled) and Rac GTPases. Consistent with this model, polarized UNC-40 within the HSN neuron in *C. elegans* is known to recruit another downstream effector, MIG-10 (lamellipodin), a protein requiring phosphoinositides modified at the 3′ position for membrane targeting[14].

Netrins have not previously been implicated in regulating cell invasions *in vivo*. Recent work, however, has shown that netrin-1 is strongly associated with metastatic breast cancer, and stimulates invasion through collagen type I gels in colon cancer cells *in vitro*[22,23]. Furthermore, netrins are potent angiogenic factors in vertebrates[24–26], a process that depends on capillary sprouts invading through the basement membrane[27]. Our observations demonstrating a direct role for UNC-6 promoting cell invasion through the basement membrane *in vivo* suggest that it is a conserved regulator of this process, and highlights the therapeutic potential of targeting netrin signalling to modulate cell-invasive behaviour. □
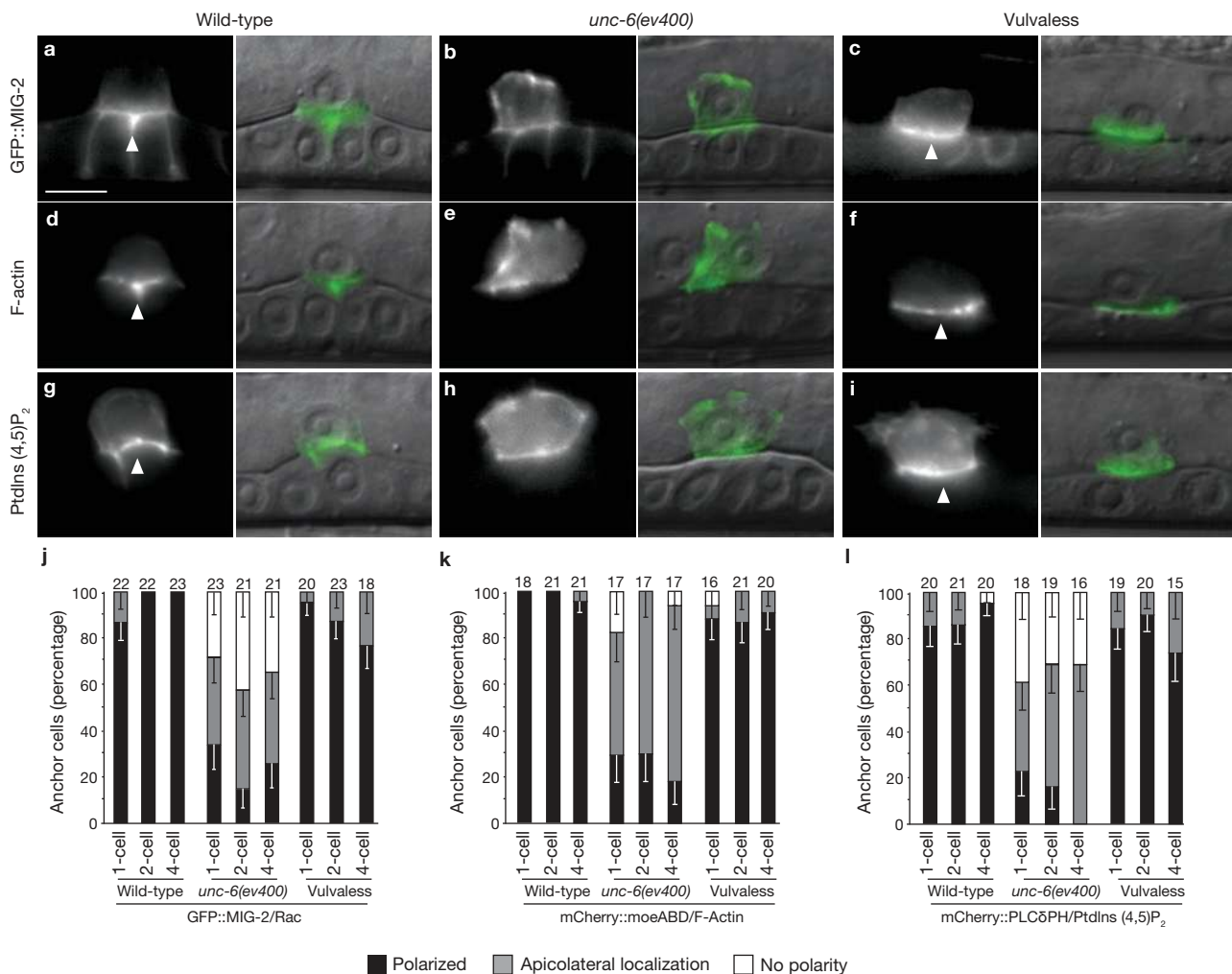
Figure 4 UNC-6 localizes the Rac protein MIG-2, F-actin and PI(4,5)P$_2$ to the invasive cell membrane. (**a**–**i**) Fluorescence image (left), Nomarski overlaid image (right). (**a**, **d**, **g**) The Rac protein GFP::MIG-2, the F-actin binding protein mCherry::moeABD and the phosphatidylinositol 4,5-bisphosphate sensor mCherry::PLCδ^{PH} were localized to the invasive cell membrane in wild-type animals (arrowheads). The endogenous *mig-2* promoter also drove low levels of expression in the vulval cells. (**b**, **e**, **h**) In *unc-6* mutants, MIG-2, F-actin and PtdIns(4,5)P$_2$ failed to polarize to the invasive cell membrane. (**c**, **f**, **i**) In contrast, MIG-2, F-actin and PtdIns(4,5)P$_2$ were polarized normally in vulvaless animals (arrowheads). (**j**, **k**, **l**) Quantification of MIG-2, F-actin and PtdIns(4,5)P$_2$ polarization, respectively, in wild-type, *unc-6,* and vulvaless animals before and during invasion. Localization of all markers was significantly perturbed in *unc-6* animals at all time-points examined, compared with wild-type controls ($P < 0.0003$ in all cases). In contrast, vulvaless animals showed no significant changes in polarity ($P > 0.05$). The number of animals examined at each stage is noted at the top of each bar; error bars show s.e.m. of the proportion and raw percentages are reported in Supplementary Information, Table S3.

METHODS

Worm handling and strains. Wild-type nematodes were strain N2. Strains were reared and viewed at 20ºC or 25ºC using standard techniques. In the text and figures we refer to linked DNA sequences that code for a single fusion protein using a (::) annotation. For designating linkage to a promoter we use a (>) symbol. The following alleles and transgenes were used: *qyEx78[Venus::unc-6(ΔSP)]*, *ghEx11[egl-17>rde-1::mRFP]*, *ghEx13[egl-17>Venus::unc-6]*, *ghEx18[glr-1>Venus::unc-6]*, *qyEx60[fos-1a>mCherry:: PLCδ^{PH}]*, *qyIs25[cdh-3>mCherry:: PLCδ^{PH}]*, *qyIs61[cdh-3>GFP::unc-34]*, *qyIs67[cdh-3>unc-40::GFP]*, *syIs157[cdh-3>YFP]*, *zuIs20(par-3::GFP)*; LGI, *muIs27[GFP::mig-2]*, *unc-40(e271)*; LGII, *qyIs17[zmp-1>mCherry]*, *qyIs23[cdh-3>mCherry:: PLCδ^{PH}]*, *rrf-3(pk1426)*, *syIs77[zmp-1>YFP]*; LGIII, *ghIs8[Venus::unc-6]*, *unc-119(ed4)*, *pha-1(e2123ts)*, *rhIs23[hemicentin::GFP]*, *syIs129[hemicentin-ΔSP::GFP]*; LGIV, *ced-10(n1993)*, *jcIs1[ajm-1::GFP]*, *lin-3(n1079)*, *lin-3(n378)*; LGV, *fos-1(ar105)*, *rde-1(ne219)*, *unc-34(gm104)*, *qyIs50[cdh-3>mCherry::moeABD]*; LGX, *qyIs66[cdh-3>unc-40::GFP]*, *qyIs7[lam-1::GFP]*, *qyIs24[cdh-3>mCherry::PLCδ^{PH}]*, *syIs59[egl-17>CFP]*, *kyIs299[hs>unc-6::HA; unc-86>myr-GFP; odr-1>DsRed]*, *syIs50(cdh-3::GFP)*,

mig-2(mu28), unc-6(ev400). Vulvaless animals were created either through laser ablation or using the strain *lin-3(n1059)/lin-3(n378)*, as described previously[5]. The *hs>unc-6::HA* transgenic worms (*kyIs299*) were grown at 15ºC, conditions where it has been shown that UNC-6::HA expression is not detectable[14]. High levels of UNC-6::HA were induced with a 2 h heat shock at 30ºC as previously shown[14]. A list of additional alleles examined is available in Supplementary Information, Table S1.

Molecular biology and the generation of transgenic animals. Translational reporter constructs fusing coding sequences for GFP to the cDNAs encoding UNC-40 (*pUnc86>unc-40::GFP*), UNC-34 (*pUnc86> GFP::unc-34*), laminin (pGK41) and CED-10 (pPR80) have been described previously[14,16,28]. To label F-actin, we created construct pJWZ6 by inserting a previously described *in vivo* actin-binding probe from *Drosophila melanogaster* moesin[17] into a *Bam*H1 site 3′ to the coding sequences for mCherry (pAA64). A probe for PtdIns(4,5)P$_2$ (construct pAA173) was generated by cloning the PH domain of human PLCδ 1 (amino acids 9–139) into a *Spe*I site 3′ to the coding sequences for mCherry. To generate a *unc-6* reporter transgene (*Venus::unc-6(ΔSP)*) that would indicate the
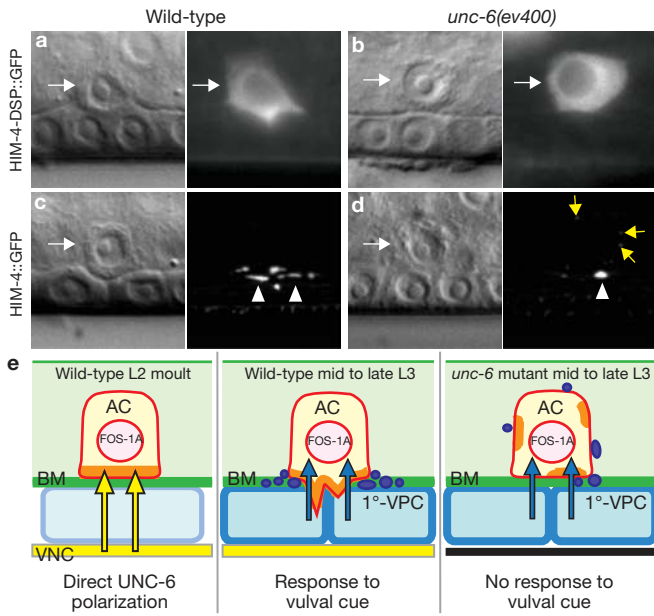
Figure 5 UNC-6 promotes the deposition of HIM-4 at the site of invasion. (**a**–**d**) Nomarski images (left) and corresponding fluorescence images (right). (**a**) Expression of the transcriptional reporter HIM-4-ΔSP::GFP within the AC (arrow) in wild-type animals during invasion. (**b**) HIM-4-ΔSP::GFP was expressed at the same levels in *unc-6* mutants ($n = 20$ for each; $P = 0.69$, unpaired t-test). (**c**) Full-length HIM-4::GFP was deposited under the invasive membrane of the AC (arrowheads) during invasion. (**d**) In *unc-6* mutants, there was a 65% reduction in HIM-4 deposition under the invasive cell membrane (arrowhead; $P = 5.0 \times 10^{-6}$, unpaired t-test), and a threefold increase in accumulations formed along apical and lateral membranes (yellow arrows; $P = 0.022$, unpaired t-test, $n = 18$ for each; Supplementary Information, Movies 1, 2). We found no significant correlation ($r^2 = -0.248$, $P = 0.320$ Students t-test, df = 16) between perturbations in HIM-4 deposition and the contact area with the basement membrane. (**e**) Diagram of the role of UNC-6 in regulating AC invasion. During the L2 moult, UNC-6 protein secreted from the ventral nerve cord (VNC and arrows in yellow) polarizes its receptor UNC-40 to the AC's plasma membrane in contact with the basement membrane (BM, green). There, UNC-40 establishes a specialized invasive membrane domain (orange) containing F-actin, and its effectors — actin regulators and the PtdIns(4,5)P$_2$. Approximately 4-6 h later, HIM-4 is deposited under the invasive cell membrane (puncta, purple) and invasive protrusions are generated in response to the 1°-VPCs (arrows in blue). In *unc-6* mutants, the invasive membrane is not polarized, HIM-4 deposition is reduced and mis-targeted, and the AC fails to generate invasive processes in response to the 1°-VPC signal. Importantly, this model for UNC-40 localization does not preclude the possibility of feed-back mechanisms that regulate UNC-40 localization and function.

cells in which UNC-6 message is transcribed, we modified a rescuing venus::unc-6 plasmid (*pVns-unc-6*)[11] using a PCR fusion-based strategy described previously[29]. Primers were designed such that the nucleotides encoding the predicted signal peptide (amino acids 1–21) were removed during PCR fusion.

To prepare reporter constructs for AC- or uterine-specific expression, we used PCR fusion to place each coding region into the context of a tissue-specific promoter, as previously described[8]. For uterine-specific expression we used the *fos-1a* promoter[8] and for AC-specific expression we used the AC-specific *zmp-1*[mk50-51] or *cdh-3*[mk62-63] regulatory regions[8]. We performed all fusions using either Phusion DNA polymerase (New England Biolabs) or the Expand Long Template PCR System (Roche Diagnostics). Templates and specific PCR primers for each promoter and reporter gene are listed in Supplementary Information, Table S4.

Transgenic worms are created by transformation with co-injection markers pPD no. MM016B (*unc-119*+), pBX (*pha-1*+) or pPD132.102 (*myo-2>YFP*) into the germline of *unc-119(ed4)*, *pha-1(e2123ts)* or wild-type animals, respectively.

These markers were injected with either *Eco*RI-digested salmon sperm DNA, pBluescript II or genomic *C. elegans* DNA at 40–100 ng μl^{-1} to act as a carrier DNA along with serial dilutions of the expression constructs to optimize expression levels and avoid toxicity. Transgenic extrachromosal (Ex) lines and integrated strains (Is) generated in this study are listed in Supplementary Information, Table S5. Integrated strains were generated as described previously[8].

Image acquisition, processing and analysis. Images were acquired using a Zeiss AxioImager A1 microscope with a ×100 plan-apochromat objective and a Zeiss AxioCam MRm CCD camera, controlled by Zeiss Axiovision software (Zeiss Microimaging), or using a Yokogawa spinning disk confocal mounted on a Zeiss AxioImager A1 microscope using IVision software (Biovision Technologies). Images were processed and overlaid using Photoshop 8.0 (Adobe Systems), and 3-dimensional projections were constructed using IMARIS 6.0 (Bitplane).

Scoring of AC invasion, polarity and fluorescence-intensity. AC invasion was scored as described previously[8]. Polarity defects of *unc-6(ev400)* animals were determined by comparing average fluorescence intensity from five-pixel-wide linescans drawn along the invasive and non-invasive membranes of UNC-40::GFP and mCherry::moeABD in wild-type and mutant strains. To generate a polarity ratio, the fluorescence density of the invasive membrane was divided by the fluorescence density of the non-invasive membrane. This analysis showed a 3.3-fold enrichment of UNC-40::GFP and a 4.0-fold enrichment of mCherry::moeABD at the invasive membranes of wild-type animals. Loss of UNC-6 significantly perturbed AC polarity, reducing the polarity ratio by more than 50% for each marker ($P = 2 \times 10^{-7}$, unpaired t-test, $n = 20$ for each marker/genotype). Similarly, ectopic expression of UNC-6 significantly reduced the polarity of UNC-40::GFP by more than 40% when compared with controls ($P = 0.006$, $n = 15$ animals for each treatment). Other markers behaved consistently with these results. Through visual inspection of many wild-type and mutant animals, however, we determined that the diversity of polarity phenotypes of *unc-6* mutant animals was more accurately conveyed by grouping them into three phenotypic categories. These are reported in the figures and were grouped as follows: ACs containing a single intense region or fluorescence signal along the basal cortex/membrane were scored as 'Polarized'; ACs with a roughly uniform distribution of fluorescence along all aspects of the cortex/membrane were scored as having 'No Polarization'; ACs observed with a significant basal region of signal and with intense accumulations along apical or lateral faces were scored as 'Apicolateral Accumulation'. In all cases, Fisher's exact test was used to determine statistical significance of these analyses.

Mean fluorescence intensity of HIM-4 deposition and AC expression of transgenic GFP reporter constructs in wild-type and *unc-6* mutants ($n = 18$ animals for each genotype) were calculated by sum-projecting confocal z series using Image J 1.40g software.

Laser ablation and P8.p isolation assay. Laser-directed cell ablations were performed on 5% agar pads, as described previously[5]. The attraction assay was carried out on strains NK212 (*syIs157[cdh-3>YFP]; syIs59[egl-17>CFP]*) and NK214 (*syIs157[cdh-3>YFP]; syIs59[egl-17>CFP] unc-6(ev400)*). AC invasion in both NK212 and NK214 without ablation produced similar results as N2 and *unc-6-(ev400)* mutants, respectively ($n = 50$ animals examined for each). Ablation of the VPCs P3.p through P7.p in both strains was performed at the early to mid L2 stage. Animals were then recovered from the agar pad used for ablation, allowed to develop at 20ºC, and then examined for AC attraction to the P8.p cell and its descendants 18-24 h after recovery.

Apical AJM-1 scoring in the AC. AJM-1::GFP localization was observed in a single nascent spot junction in the apical region of the AC in wild-type animals beginning at the late P6.p 1-cell stage, approximately 3-4 h before invasion. The number of spot junctions increased to approximately two by the P6.p 4-cell stage (range was from 1–4). The number and apical position of spot junctions was then compared in wild-type and *unc-6* mutants from the P6.p 1-cell stage through the P6.p 4-cell stage.

RNA interference. Double-stranded RNA (dsRNA) against *fos-1* was delivered by feeding as described previously[8]. To trigger vulval-cell-specific knockdown of *unc-6* expression, *rde-1(ne219); ghEx11[egl-17>rde-1::mRFP]*,worms were cultured on bacteria-generating dsRNA, targeting *unc-6*[11].

Note: Supplementary Information is available on the Nature Cell Biology website.

1. Machesky, L., Jurdic, P. & Hinz, B. Grab, stick, pull and digest: the functional diversity of actin-associated matrix-adhesion structures. Workshop on invadopodia, podosomes and focal adhesions in tissue invasion. *EMBO Rep.* **9**, 139–143 (2008).
2. Even-Ram, S. & Yamada, K. M. Cell migration in 3D matrix. *Curr. Opin. Cell Biol.* **17**, 524–532 (2005).
3. Hotary, K., Li, X. Y., Allen, E., Stevens, S. L. & Weiss, S. J. A cancer cell metalloprotease triad regulates the basement membrane transmigration program. *Genes Dev.* **20**, 2673–2686 (2006).
4. Sharma-Kishore, R., White, J. G., Southgate, E. & Podbilewicz, B. Formation of the vulva in *Caenorhabditis elegans*: a paradigm for organogenesis. *Development* **126**, 691–699 (1999).
5. Sherwood, D. R. & Sternberg, P. W. Anchor cell invasion into the vulval epithelium in *C. elegans*. *Dev. Cell* **5**, 21–31 (2003).
6. Hwang, B. J., Meruelo, A. D. & Sternberg, P. W. *C. elegans* EVI1 proto-oncogene, EGL-43, is necessary for Notch-mediated cell fate specification and regulates cell invasion. *Development* **134**, 669–679 (2007).
7. Rimann, I. & Hajnal, A. Regulation of anchor cell invasion and uterine cell fates by the egl-43 Evi-1 proto-oncogene in *Caenorhabditis elegans*. *Dev. Biol.* **308**, 187–195 (2007).
8. Sherwood, D. R., Butler, J. A., Kramer, J. M. & Sternberg, P. W. FOS-1 promotes basement-membrane removal during anchor-cell invasion in *C. elegans*. *Cell* **121**, 951–962 (2005).
9. Baker, K. A., Moore, S. W., Jarjour, A. A. & Kennedy, T. E. When a diffusible axon guidance cue stops diffusing: roles for netrins in adhesion and morphogenesis. *Curr. Opin. Neurobiol.* **16**, 529–534 (2006).
10. Hedgecock, E. M., Culotti, J. G. & Hall, D. H. The *unc-5*, *unc-6*, and *unc-40* genes guide circumferential migrations of pioneer axons and mesodermal cells on the epidermis in *C. elegans*. *Neuron* **4**, 61–85 (1990).
11. Asakura, T., Ogura, K. & Goshima, Y. UNC-6 expression by the vulval precursor cells of *Caenorhabditis elegans* is required for the complex axon guidance of the HSN neurons. *Dev. Biol.* **304**, 800–810 (2007).
12. Wadsworth, W. G., Bhatt, H. & Hedgecock, E. M. Neuroglia and pioneer neurons express UNC-6 to provide global and local netrin cues for guiding migrations in *C. elegans*. *Neuron* **16**, 35–46 (1996).
13. Burdine, R. D., Branda, C. S. & Stern, M. J. EGL-17(FGF) expression coordinates the attraction of the migrating sex myoblasts with vulval induction in *C. elegans*. *Development* **125**, 1083–1093 (1998).
14. Adler, C. E., Fetter, R. D. & Bargmann, C. I. UNC-6/netrin induces neuronal asymmetry and defines the site of axon formation. *Nature Neurosci.* **9**, 511–518 (2006).
15. Gitai, Z., Yu, T. W., Lundquist, E. A., Tessier-Lavigne, M. & Bargmann, C. I. The netrin receptor UNC-40/DCC stimulates axon attraction and outgrowth through enabled and, in parallel, Rac and UNC-115/AbLIM. *Neuron* **37**, 53–65 (2003).
16. Lundquist, E. A., Reddien, P. W., Hartwieg, E., Horvitz, H. R. & Bargmann, C. I. Three *C. elegans* Rac proteins and several alternative Rac regulators control axon guidance, cell migration and apoptotic cell phagocytosis. *Development* **128**, 4475–4488 (2001).
17. Edwards, K. A., Demsky, M., Montague, R. A., Weymouth, N. & Kiehart, D. P. GFP-moesin illuminates actin cytoskeleton dynamics in living tissue and demonstrates cell shape changes during morphogenesis in *Drosophila*. *Dev. Biol.* **191**, 103–117 (1997).
18. Janmey, P. A. & Lindberg, U. Cytoskeletal regulation: rich in lipids. *Nature Rev. Mol. Cell Biol.* **5**, 658–666 (2004).
19. Heo, W. D. *et al*. PI(3, 4, 5)P3 and PI(4, 5)P2 lipids target proteins with polybasic clusters to the plasma membrane. *Science* **314**, 1458–1461 (2006).
20. Rescher, U., Ruhe, D., Ludwig, C., Zobiack, N. & Gerke, V. Annexin 2 is a phosphatidylinositol (4, 5)-bisphosphate binding protein recruited to actin assembly sites at cellular membranes. *J. Cell Sci.* **117**, 3473–3480 (2004).
21. Colon-Ramos, D. A., Margeta, M. A. & Shen, K. Glia promote local synaptogenesis through UNC-6 (netrin) signalling in *C. elegans*. *Science* **318**, 103–106 (2007).
22. Fitamant, J. *et al*. Netrin-1 expression confers a selective advantage for tumour cell survival in metastatic breast cancer. *Proc. Natl Acad. Sci. USA* **105**, 4850–4855 (2008).
23. Rodrigues, S., De Wever, O., Bruyneel, E., Rooney, R. J. & Gespach, C. Opposing roles of netrin-1 and the dependence receptor DCC in cancer cell invasion, tumour growth and metastasis. *Oncogene* **26**, 5615–5625 (2007).
24. Nguyen, A. & Cai, H. Netrin-1 induces angiogenesis via a DCC-dependent ERK1/2-eNOS feed-forward mechanism. *Proc. Natl Acad. Sci. USA* **103**, 6530–6535 (2006).
25. Park, K. W. *et al*. The axonal attractant Netrin-1 is an angiogenic factor. *Proc. Natl Acad. Sci. USA* **101**, 16210–16215 (2004).
26. *Wilson*, B. D. *et al*. Netrins promote developmental and therapeutic angiogenesis. *Science* **313**, 640–644 (2006).
27. Heissig, B., Hattori, K., Friedrich, M., Rafii, S. & Werb, Z. Angiogenesis: vascular remodelling of the extracellular matrix involves metalloproteinases. *Curr. Opin. Haematol.* **10**, 136–141 (2003).
28. Kao, G., Huang, C. C., Hedgecock, E. M., Hall, D. H. & Wadsworth, W. G. The role of the laminin beta subunit in laminin heterotrimer assembly and basement membrane function and development in C. elegans. *Dev. Biol.* **290**, 211–219 (2006).
29. Hobert, O. PCR fusion-based approach to create reporter gene constructs for expression analysis in transgenic C. elegans. *Biotechniques* **32**, 728–730 (2002).

nature cell biology

DOI: 10.1038/ncb1825
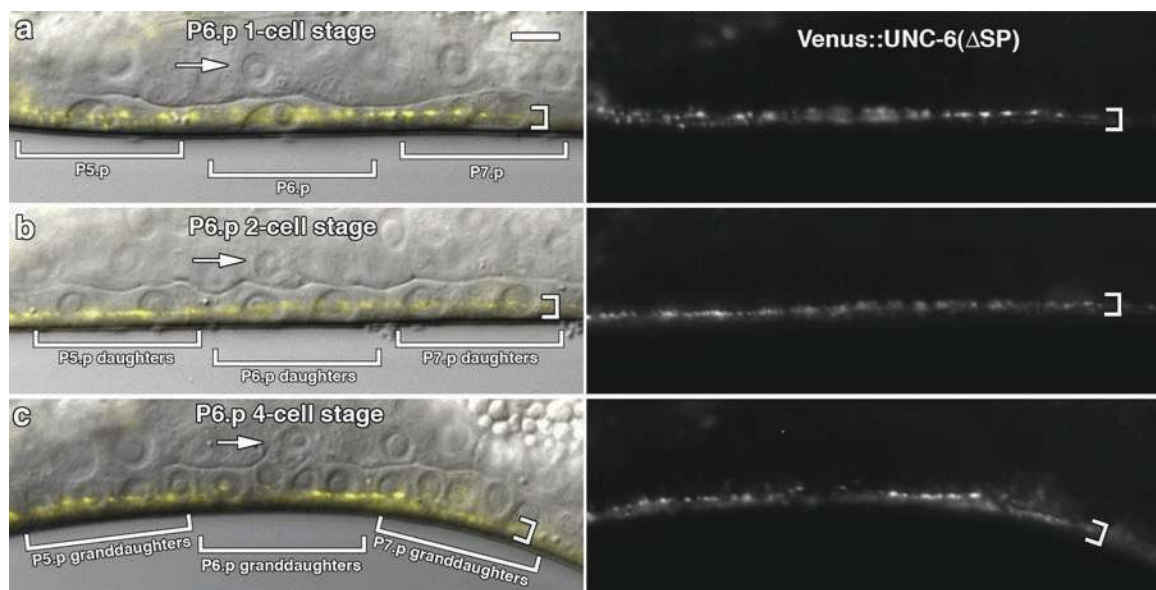
Figure S1 Venus::UNC-6 expression prior to and during AC invasion. **(a-c)** Nomarski images overlayed with Venus::UNC-6 (ΔSP) expression shown in yellow (left), and Venus::UNC-6 (ΔSP) fluorescence alone (right). Venus::UNC-6 (ΔSP) lacks a signal sequence and was thus retained in the cells in which *unc-6* is expressed. Venus::UNC-6 was retained within the neurons of the ventral nerve cord (VNC, small bracket) under the AC (arrow) prior to invasion at the P6.p 1- and 2-cell stages (large brackets, **a** and **b**), and during the time of invasion at constant levels (**c**). Scale bar in (**a**) is 5μm in this and all subsequent supplementary figures.
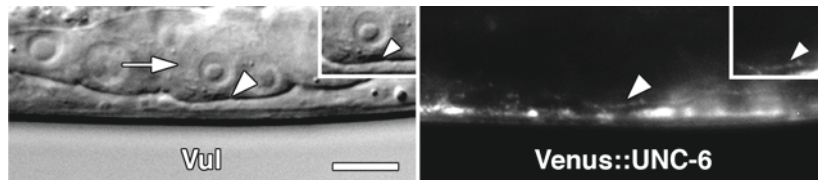
Figure S2 Venus::UNC-6 expression and localization is not dependent on the vulval cells. Nomarski image (left), and corresponding fluorescence image (right) of an animal expressing Venus::UNC-6 at the early L3 stage after laser-mediated ablation of the vulval cells in the early L2 larval stages. Venus::UNC-6 was expressed normally in the VNC and localized to the basement membrane (arrowhead) under the AC (arrow) as in wild-type animals (n = 24/24 animals). Inset highlights the basement membrane localization of Venus::UNC-6 (arrowhead) under the AC.
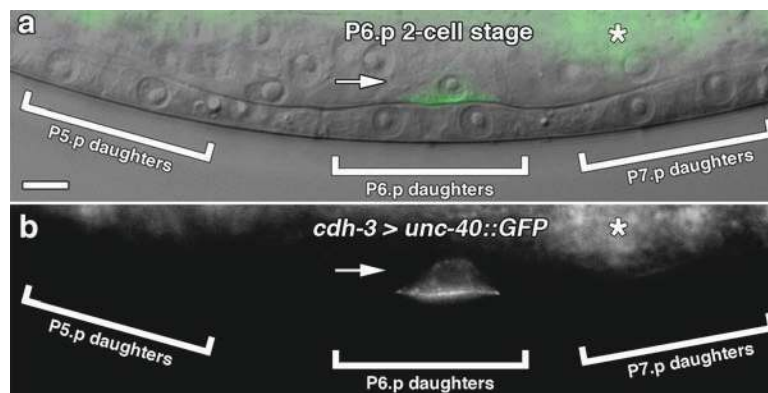
Figure S3 AC-specific expression of UNC-40::GFP. (**a**) Nomarski image overlayed with UNC-40::GFP fluorescence (green). The *unc-40::GFP* construct is driven by the AC-specific regulatory element of the *cdh-3* gene. (**b**) The corresponding fluorescence image of UNC-40::GFP fluorescence alone. The *cdh-3* AC-specific promoter drives expression solely in the AC (arrow), and not in neighboring cells, including vulval cells (brackets). The asterisk marks autofluorescence from the gut granules.
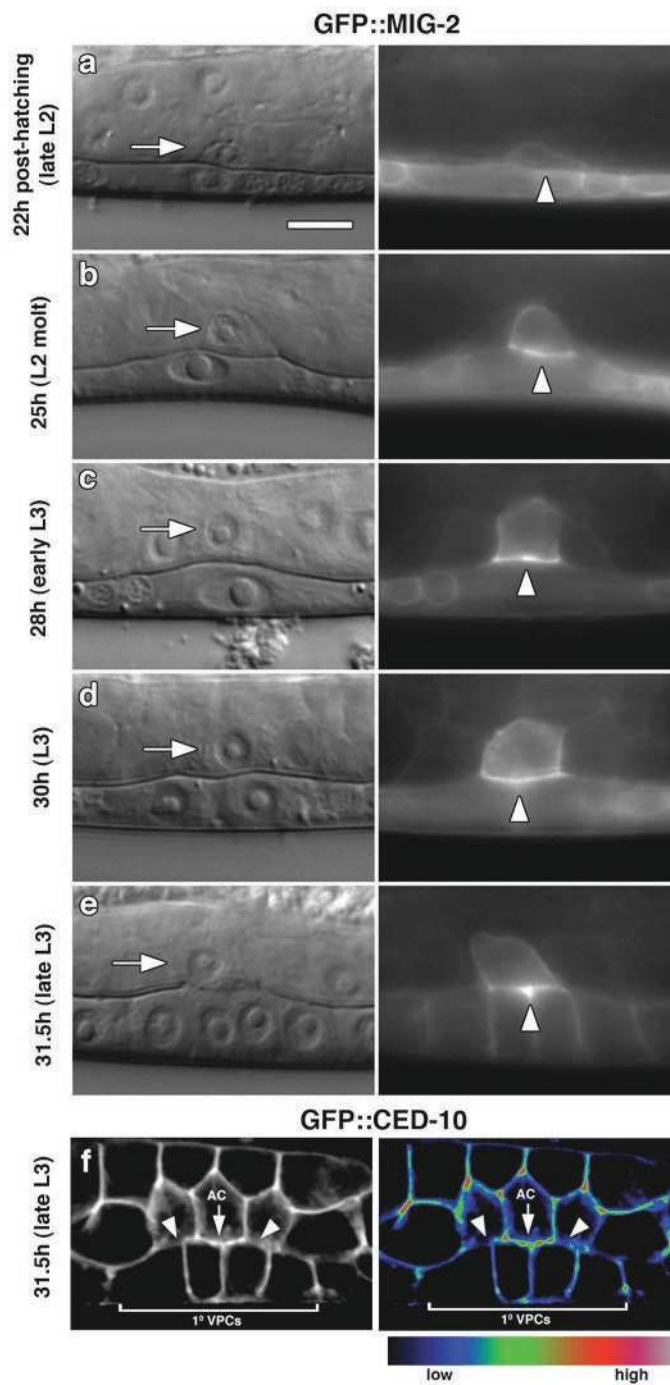
Figure S4 The Rac orthologs GFP::MIG-2 and GFP::CED-10 are polarized along the invasive cell membrane of the AC. **(a-e)** Nomarski images (left), corresponding fluorescence images (right). Time is post-hatching at 20ºC. **(a)** GFP::MIG-2 expression driven by its endogenous promoter was first expressed in the AC during the late L2 (9.5 hours before invasion) and was not polarized (16/16 animals). **(b)** MIG-2 was first polarized at the L2 molt (arrowhead; 7/11 animals). **(c-e)**. Polarized MIG-2 was maintained along the invasive cell membrane from the early L3 stage through the time of invasion (20/20 animals for each stage). **(f)** Projected confocal z-stack showing uterine and vulval expression of GFP::CED-10 driven by its endogenous promoter (left) and the corresponding spectral representation of the fluorescence intensity (right). CED-10 was expressed in all uterine and vulval cells (bracket outlines the 1º VPCs), and was polarized along the basal (invasive) membrane of the AC (arrow) but not in neighboring uterine cells (arrowheads).
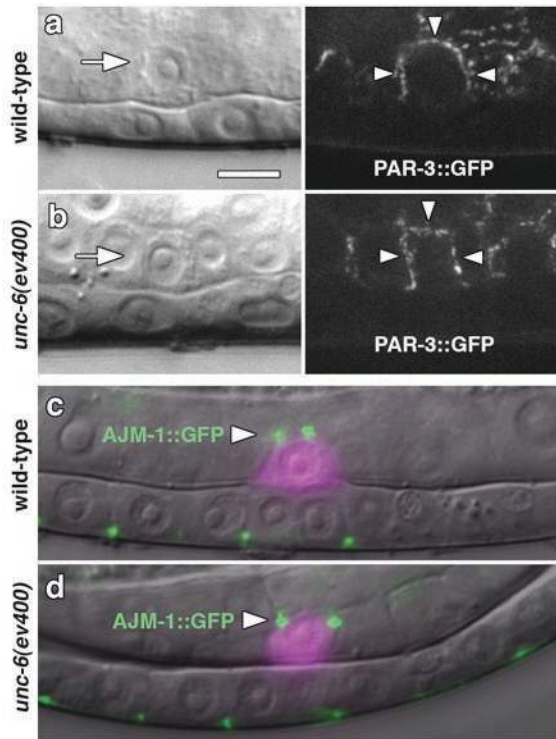
Figure S5 PAR-3::GFP and apical AJM-1::GFP are localized normally in *unc-6* mutants. (**a**, **b**) Nomarski images (left), corresponding fluorescence images (right). (**a**) PAR-3::GFP was localized to apical and lateral membranes of wild-type ACs prior to invasion (arrowheads), and this polarity was not altered in *unc-6* mutants (**b**, arrowheads; *n* = 20/20 animals). (**c**) In wild-type animals AJM-1::GFP (green) localized to nascent junctions (arrowhead) in the apical region of the AC (expressing *zmp-1>mCherry* in magenta). (**d**) In *unc-6* mutants apical AJM-1::GFP junctions were formed and positioned normally compared to wild-type animals (*n* ≥ 60 wild-type and *unc-6* animals examined).
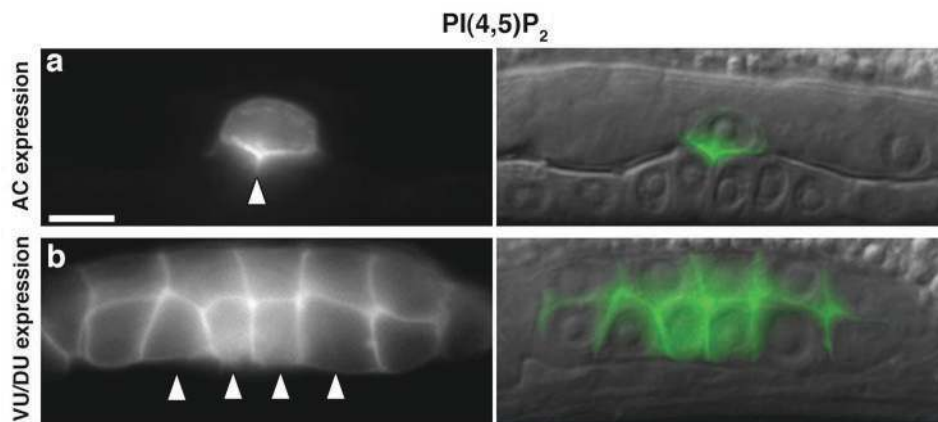
Figure S6 Pan-uterine expression of mCherry:: PLCδ^{PH} reveals a unique PI(4,5)P$_2$ rich invasive membrane domain in the AC. Fluorescence (left) overlaid on corresponding Normarski image (right). (**a**) Expression of the PI(4,5)P$_2$ sensor mCherry::PLCδ^{PH} in the AC revealed strong polarization at the basal (invasive) cell membrane (arrowhead). (**b**) In contrast, a section lateral to the AC through the neighboring ventral and dorsal uterine cells (VU/DU) expressing PLCδ^{PH}::mCherry, revealed that adjacent uterine cells did not have PI(4,5)P$_2$ concentrated in basal membranes (arrowheads).
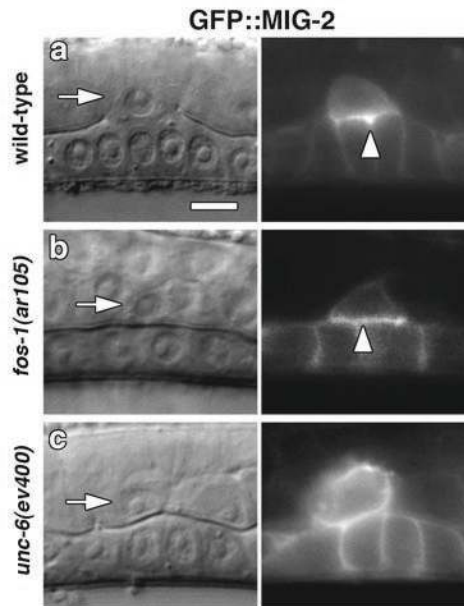
Figure S7 GFP::MIG-2 is localized normally in the AC of *fos-1(ar105)* animals. Nomarski images (left), corresponding fluorescence images (right). In (**a**) wild-type animals and (**b**) *fos-1(ar105)* mutants, MIG-2::GFP was strongly polarized to the invasive cell membrane of the AC (arrowhead; *n* = 20/20 *fos-1*a mutants examined). (**c**) In *unc-6* animals, MIG-2::GFP polarity was perturbed.

Supplementary Movie Legends

Movie S1 Hemicentin::GFP deposition under the AC in wild-type animals. Hemicentin::GFP was localized at low levels along gonadal and ventral epidermal basement membranes, but was deposited at high levels (green, orange arrows) under the AC's invasive cell membrane (expressing *cdh-3*>mCherry::moeABD in magenta) during AC invasion. Little hemicentin::GFP was deposited along apical or lateral domains of the AC (note small deposit at white arrowhead).

Movie S2 Hemicentin::GFP deposition is perturbed *unc-6* mutants. In *unc-6* mutants there was a dramatic decrease in hemicentin deposited under the AC (expressing *cdh-3*>mCherry::moeABD in magenta) at the site of basement membrane contact (green, orange arrows), while apical and lateral accumulations of hemicentin increased (white arrowheads).

Table S1. AC invasion in mutant strains with roles in cell motility and axon outgrowth

C. elegans gene	Encoded Product	Invasion at P6.p 4-cell stage (number of ACs invaded/number observed)[a]	Invasion at P6.p 8-cell stage (number of ACs invaded/number observed)
arf-1.2(ok796)	ADP-ribosylation factor 1 homolog	10/10	10/10
arf-1.2(ok1322)	ADP-ribosylation factor 1 homolog	9/9	4/4
bar-1 (ga80)	Armadillo/beta-Catenin/plakoglobin	11/11	9/9
C25F6.4(ok874)	protein tyrosine kinase homolog that is also homologous to human RS1	15/15	16/16
cam-1(gm122)	receptor tyrosine kinase of the immunoglobulin superfamily that is orthologous to human ROR1	7/9	28/35
cam-2(gm124)	uncloned locus that affects migration of canal associated neurons	6/6	5/5
cdh-4(ok1323)	member of the cadherin superfamily	10/10	8/8
cdh-5(hc181)	member of the cadherin superfamily	10/10	7/7
cdh-7(ok428)	contains a cadherin domain	10/10	not observed
ced-2(e1752)	Src homology (SH) 2 and 3-containing adaptor protein	10/10	11/11
ced-5(n1812)	homolog of the human protein DOCK180	10/10	13/13
ced-12(k149)	Regulator of Rac1, required for phagocytosis and cell migration	11/11	12/12
ceh-10(ct78)	Paired-like class of homeodomain proteins	10/10	8/8
ces-1(n1414)	C2H2-type zinc finger transcription factor that is a member of the Snail family of proteins	11/11	11/11
ces-1(n703)	C2H2-type zinc finger transcription factor that is a member of the Snail family of proteins	16/16	14/14
cle-1(cg120)	collagen protein with endostatin domain	9/9	13/13
crb-1(ok931)	homolog of Drosophila CRUMBS	9/9	9/9
daf-1(m40)	TGF-beta type I receptor homolog	8/9	6/6
daf-4(e1364)	type II transforming growth factor-beta (TGF-b) receptors	11/11	14/14
daf-7(e1372)	member of the transforming growth factor beta (TGFbeta) superfamily	12/12	14/14
dgn-2(ok209)	dystroglycan	27/27	20/20
dbl-1(wk70)	member of the transforming growth factor beta (TGFbeta) superfamily	21/21	6/6
dpy-19(e1295)	novel transmembrane protein	7/7	7/7
efn-4(bx80)	member of the ephrin family of ligands	10/10	17/17
egl-15(MT3324)	FGF-like receptor tyrosine kinase	13/13	7/7
egl-17(e1313)	fibroblast growth factor-like protein	13/13	8/8
evl-20(ar103)	a functional ortholog of human ADP-ribosylation factor-like protein 2	not observed	4/4
F11D5.3(ok574)	a putative tyrosine kinase homologous to human RS1	11/11	22/22
flt-1(ok722)	a putative homolog of flectin, an extracellular matrix protein	10/10	8/8
gon-1(e1254)/eDf18	a functional metalloprotease that defines a new sub-family of secreted proteases known as MPT (metalloprotease with thrombospondin type 1 repeats)	8/8	11/11
gpn-1(ok377)	glypican, a heparan sulfate proteoglycan anchored to the cell membrane by a GPI linkage	13/13	14/14
hlh-8(nr2061)	helix-loop-helix protein required for normal muscle development	10/10	18/18
lad-1(ok1244)/sax-7	ortholog of human L1CAM	10/10	13/13
let-756(S2613)	fibroblast growth factor (FGF)-like ligand	9/11	21/21
lon-2(e678)	member of the glypican family of heparan sulfate proteoglycans	13/13	19/19
mab-20 (ev574)	semaphorin	9/10	13/13
mab-20(bx24)	semaphorin	10/10	10/10
max-1(ju39)	conserved PH/MyTH4/FERM domain-containing protein	15/15	10/10
mig-1(e1787)	Frizzled-like receptor	10/10	13/13
mig-2(gm103)	Rho family of GTP-binding proteins, similar to Rac	12/15	36/37
mig-6(e1931)	uncloned locus involved in cell migration	9/10	15/15
mig-14(ga62)	homologous to drosophila Wntless	10/10	15/15
mig-15(rh326)	Nck-interacting kinase (NIK)	8/9	10/10
mig-17(k113)	secreted metalloprotease that is a member of the ADAM (A Disintegrin And Metalloprotease) protein family	10/10	13/13

mom-2(or42)	member of the Wnt family of secreted signaling glycoproteins	6/6	20/20
mom-5(or57)	Frizzled-like receptor	2/5	7/8
pkc-3(RNAi)	Serine/threonine protein kinase, atypical Protien Kinase C	15/15	no data
pld-1(ok986)	phospholipase D1	10/10	2/2
plx-1(nc37)	plexin ortholog, semaphorin receptor	10/10	10/10
ptp-3(op147)	receptor-like tyrosine phosphatase	10/10	15/15
qid-7(mu533)	uncloned locus that affects Q neuroblast polarization and migration	11/11	10/10
qid-8(mu342)	uncloned locus that affects Q neuroblast polarization and migration	10/10	13/15
rac-2(ok326)	Rho family GTPase that is one of three C. elegans Rac-related proteins	10/10	7/7
rig-4(ok1160)	Immunoglobulin C-2 Type/fibronectin type III domains	10/10	5/5
sax-3(ky123)	homologous to Drosophila roundabout	11/11	10/10
sdn-1(ok449)	a type I transmembrane heparan sulfate proteoglycan, syndecan	13/13	5/5
slt-1(eh15)	homolog of Drosophila slit	16/16	11/11
slt-1(ok255)	homolog of Drosophila slit	80/81	59/59
sma-6(wk7)	serine/threonine protein kinase that is orthologous to type I TGF-beta receptors	10/10	15/15
smp-1 (ev715)	semaphorin	10/11	12/12
smp-2 (ev709)	semaphorin	10/10	10/10
syg-1(ky652)	a novel transmembrane protein	9/9	12/12
syg-2(ky671)	transmembrane protein, immunoglobulin superfamily	10/10	4/4
tag-150(gk261)	Guanine nucleotide exchange factor for Rho and Rac GTPases	10/10	11/11
unc-3(e151)	a protein with homology to immunoglobulin (Ig) domain-containing transcription factors	10/10	10/10
unc-5(e53)	a netrin receptor required for dorsal cell and axon migration	10/10	22/22
unc-6(ev400)	netrin ortholog, secreted guidance molecule that regulates pioneer axons and mesodermal cells	4/20	14/18
unc-14(e57)	an activity required for both axonogenesis and sex myoblast migration	8/10	11/11
unc-18(e81)	an ortholog of Saccharomyces cervisiae SEC1	10/11	12/12
unc-30(e191)	Pitx homeodomain transcription factor family member	10/10	10/10
unc-33(mn407)	CRMP/TOAD/Ulip/DRP homologue	10/10	10/11
unc-34(e315)	EVH1 domain-containing protein that is the sole C. elegans Enabled/VASP homolog	6/10	12/12
unc-34(e566)	EVH1 domain-containing protein that is the sole C. elegans Enabled/VASP homolog	5/8	5/5
unc-39(e257)	homeodomain transcription factor that belongs to the Six4/5 family	10/10	11/11
unc-40(e271)	A netrin receptor required for guiding dorsal and ventral cell and axon migrations	6/21	13/18
unc-44(e1197)	ankyrin-like protein	10/10	10/10
unc-44(e362)	ankyrin-like protein	10/10	2/2
unc-51 (e369)	serine/threonine kinase involved in autophagy	9/10	13/13
unc-51(e1189)	serine/threonine kinase involved in autophagy	10/12	10/10
unc-53(e404)	orthologous to human NAV1, NAV2/RAINB1, and NAV3	11/11	7/7
unc-53(n152)	orthologous to human NAV1, NAV2/RAINB1, and NAV3	10/10	13/13
unc-60(e723)	orthologs of actin depolymerizing factor/cofilin	15/15	16/16
unc-60(su158)	orthologs of actin depolymerizing factor/cofilin	37/39	30/30
unc-71 (e541)	ADAM, a disintegrin and metalloprotease-containing transmembrane protein	10/10	10/10
unc-73 (e936)	guanine nucleotide exchange factor (GNEF) similar to the trio protein	not observed	39/39
unc-73 (gm40)	guanine nucleotide exchange factor (GNEF) similar to the trio protein	6/11	22/22
unc-76(e911)	coiled-coil protein that belongs to the FEZ (fasciculation and elongation protein; zygin/zeta-1) family of proteins	9/11	10/10
unc-78(gk27)	homolog of actin-interacting protein 1	26/26	27/27
unc-97(su10)	LIM domain-containing protein of the PINCH family	10/10	14/14
unc-115(e2225)	Actin-binding LIM Zn-finger protein Limatin involved in axon guidance	10/10	15/15
unc-115(ky275)	Actin-binding LIM Zn-finger protein Limatin involved in axon guidance	67/67	68/68
unc-115(mn481)	Actin-binding LIM Zn-finger protein Limatin	8/11	24/24
unc-129 (ev554)	member of the transforming growth factor beta (TGFbeta) superfamily	5/5	11/11

vab-1(e2)	ephrin receptor	10/10	10/10
vab-8(e1017)	novel protein containing an atypical kinesin-like motor domain	10/10	10/10
vab-9(e1744)	claudin homolog	8/9	13/13
ver-1(ok859)	Fibroblast/platelet-derived growth factor receptor and related receptor tyrosine kinases	10/10	4/4
ver-2(ok897)	Fibroblast/platelet-derived growth factor receptor and related receptor tyrosine kinases	10/10	8/8
ver-3(gk227)	Fibroblast/platelet-derived growth factor receptor and related receptor tyrosine kinases	11/11	13/13
ver-4(ok1079)	Fibroblast/platelet-derived growth factor receptor and related receptor tyrosine kinases	10/10	5/5
zig-1(ok784)	secreted 2-immunoglobulin-domain protein	9/9	5/5
zig-2(ok696)	secreted 2-immunoglobulin-domain protein	9/9	11/11
zig-3(gk33)	secreted 2-immunoglobulin-domain protein	10/10	4/4
zig-4(gk4)	secreted 2-immunoglobulin-domain protein	10/10	4/4
zig-5(ok1065)	secreted 2-immunoglobulin-domain protein	11/11	10/10
zig-6(ok723)	secreted 2-immunoglobulin-domain protein	10/10	3/3
zig-8(ok561)	secreted 2-immunoglobulin-domain protein	9/9	4/4

[a] ACs showing any degree of invasion were scored as invaded and invasion was scored over the entire range of the 4-cell stage, including the L3 molt. In contrast, Table S2 4-cell stage animals were only scored at beginning of the 4-cell stage at the mid-to-late L3 stage, and partial invasions were scored.

Table S2. Timing and degree of AC invasion into the vulval epithelium

Genotype/Treatment	ACs showing full, partial or no invasion							
	P6.p 4-cell stage (mid-to-late L3 stage)				P6.p 8-cell stage (early L4 stage)			
	% Full Invasion	% Partial Invasion	% No Invasion	n =	% Full Invasion	% Partial Invasion	% No Invasion	n =
wild-type (N2)	100	0	0	>100	100	0	0	>100
unc-6/site of action								
unc-6(ev400)	0	26	74	54	52	26	22[h]	54
ghIs8[unc-6>Venus::unc-6]; unc-6(ev400)[a]	91	4	5	55	100	0	0	53
unc-6(ev400); ghEx15[glr-1p>Venus::unc-6; tph-1p>GFP][b]	90	4	6	50	96	4	0	50
unc-6(ev400);ghEx13[egl-17>Venus::unc-6][c]	8	22	70	50	60	16	25	58
rde-1(ne219);ghEx11[egl-17>rde1::mRFP]; unc-6(RNAi)[d]	100	0	0	51	100	0	0	34
lin-3(n1059)/lin-3(n378) (Vul)[e]	21	0	79	52	19	0	81[i]	52
lin-3(n1059)/lin-3(n378);unc-6(ev400)	0	0	100	50	0	0	100[j]	50
laser killed P3.p-P8.p(Vul); unc-6(ev400)	0	0	100	20	0	0	100[k]	20
kyIs299 [hs>unc-6::HA][f]	50	26	24	50	nd	nd	nd	nd
N2(mock heat shock)	98	2	0	51	nd	nd	nd	nd
Netrin receptors/*unc-40*/site of action								
unc-40(e271)	2	31	67	54	58	25	17[l]	53
unc-40(e271); unc-6(ev400)	2	29	69	51	57	21	21[m]	70
unc-40(e271); qyIs66[cdh-3>unc-40::gfp]	96	2	2	54	98	2	0	53
unc-5(e51)	100	0	0	58	100	0	0	64
Intracellular effectors								
mig-10(ct41)	100	0	0	59	100	0	0	81
ced-10(n1993)	98	2	0	61	100	0	0	57
mig-2(mu28)	100	0	0	54	100	0	0	64
ced-10(n1993); mig-2(mu28)	24	10	66	29	69	5	25	55
unc-34(gm104)	64	16	20	50	100	0	0	50
qyIs23(cdh-3>mCherry::PLCδ^{PH})[g]	85	13	2	55	100	0	0	50
qyIs23(cdh-3>mCherry::PLCδ^{PH}); mig-2(mu28)		18	12	114	99	1	0	110
qyIs23(cdh-3>mCherry::PLCδ^{PH}); unc-34(gm104)	41	18	41	51	89	9	2	56
fos-1 pathway interaction								
unc-40(e271); rrf-3(pk1426)	8	27	65	51	50	22	28	50
unc-40(e271); rrf-3(pk1426); fos-1(RNAi)	4	11	85	54	12	12	77	52
rrf-3(pk1426); fos-1(RNAi)	10	8	82	50	16	26	58	50

[a] Venus::unc-6 driven by its own promoter. [11]

[b] Ventral nerve cord specific expression of Venus::unc-6 driven by *glr-1* promoter. [11]

[c] 1º VPC specific expression of Venus::unc-6 driven by the *egl-17* promoter. [11]

[d] Targeted RNAi mediated knockdown of *unc-6* in the 1º VPCs. [11]

[e] A similar percentage of ACs have been shown to invade when vulval cells are removed by ablation. [5]

[f] 2h heat shock at 30ºC followed by 4h recovery at 15ºC.

[g] *qyIs23(cdh-3> mCherry::PLCδ^{PH})* binds and sequesters PI(4,5)P$_2$ in the AC, thus reducing its levels there.

[h-m] The number of AC's that detached from the basement membrane at the L4 stage was as follows (number of detached/number that failed to invade): h = 2/12; i =11/42; j = 47/50; k = 18/20 l = 0/9; m= 2/15.

nd = not determined

Table S3. Polarized marker localization in wild-type and mutant ACs

| Genotype | Marker | Classification of marker localization patterns in wild-type and various mutant ACs | | | | | | | | | | | |
| | | P6.p 1-cell stage | | | | P6.p 2-cell stage | | | | P6.p 4-cell stage | | | |
		Polarized (%±SE)	Apicolateral Accumulation (%±SE)	No Polarity (%±SE)	N=	Polarized (%±SE)	Apicolateral Accumulation (%±SE)	No Polarity (%±SE)	N=	Polarized (%±SE)	Apicolateral Accumulation (%±SE)	No Polarity (%±SE)	N=
wild-type	mCherry::PLCδ^{PH}	85±8	15±8	0	20	86±8	14±8	0	21	95±5	0	5±5	20
wild-type	GFP::MIG-2	86±7	13±7	0	22	100	0	0	22	100	0	0	23
wild-type	mCherry::moeABD	100	0	0	18	100	0	0	21	95±5	5±5	0	21
wild-type	UNC-40::GFP	90±7	5±5	5±5	20	100	0	0	21	90±6	10±6	0	20
unc-6(ev400)	mCherry::PLCδ^{PH}	22±10	38±12	38±12	18	15±9	53±12	32±11	19	0	69±12	31±12	16
unc-6(ev400)	mCherry::moeABD	29±11	53±12	18±10	17	29±11	71±11	0	17	18±10	76±11	6±6	17
unc-6(ev400)	UNC-40::GFP	21±10	32±11	47±12	19	5±5	42±12	53±12	20	0	25±10	75±10	20
unc-6(ev400)	GFP::MIG-2	33±11	38±11	29±10	21	14±8	43±11	43±11	21	25±10	40±11	35±11	20
Vul[a]	mCherry::PLCδ^{PH}	84±9	16±9	0	19	90±7	10±7	0	20	73±12	27±12	0	15
Vul[a]	UNC-40::GFP	94±6	6±6	0	17	86±8	14±8	0	21	94±6	6±6	0	17
Vul[a]	GFP::MIG-2	95±5	5±5	0	20	87±7	13±7	0	23	76±10	24±10	0	21
Vul[a]	mCherry::moeABD	88±9	6±6	6±6	16	86±8	14±7	0	21	90±7	10±6	0	20
hs> unc-6::HA[b]	UNC-40::GFP	nd	nd	nd	nd	nd	nd	nd	nd	33±13	33±13	33±13	15
wild-type (mock)[c]	UNC-40::GFP	nd	nd	nd	nd	nd	nd	nd	nd	93±7	7±7	0	15

[a] Vul (vulvaless) animals were of the genotype *lin-3(n1059)/lin-3(n378)*.

[b] Heat shock directed expression of *unc-6::HA* from the integrated transgene *kyIs299*, 2h heat shock at 30ºC followed by 4h recovery at 15ºC.

[c] wild-type animals expressing UNC-40::GFP in the AC were subjected to an identical experimental regimen to confirm that heat shock alone does not cause defects in UNC-40::GFP localization.

Table S4. Primer sequences and templates used for PCR fusions

Primer Sequence	Primer Type	Amplicon	Template
5' TAA TgT gAg TTA gCT CAC TCA TTA gg 3'	forward	*cdh-3/zmp-1>* promoters	*cdh-3>*, pPD107.94/mk62-63; *zmp-1>*, pPD107.94/mk50-51
5' AAC gAT ggA TAC gCT AAC AAC TTg g 3'	forward nested	*cdh-3/zmp-1>* promoters	*cdh-3>*, pPD107.94/mk62-63; *zmp-1>*, pPD107.94/mk50-51
5' TTT CTg AgC TCg gTA CCC TCC AAg 3'	reverse	*cdh-3/zmp-1>* promoters	*cdh-3>*, pPD107.94/mk62-63; *zmp-1>*, pPD107.94/mk50-51
5' TAg gCT TTT CCg TAT AgC ATC CTC 3'	forward	*fos-1a>* promoter	cosmid F29G9
5' gCC CAA CTC TAg TCA TTT CTA gC 3'	forward nested	*fos-1a>* promoter	cosmid F29G9
5' TCC ACT CTC TTA TAT AgC AgA ggT gC 3'	reverse	*fos-1a>* promoter	cosmid F29G9
5' CTT ggA ggg TAC CgA gCT Cag AAA ggT ACC Atg AgT AAA ggA gAA g 3'	*cdh-3/zmp-1* extension, forward	*GFP::unc-34*	*punc-86>GFP::unc-34*
5' Cgg gAA gCT AgA gTA AgT AgT TCg CC 3'	reverse	*GFP::unc-34*	*punc-86>GFP::unc-34*
5' CTC TCA Agg ATC TTA CCg CTg TTg 3'	reverse nested	*GFP::unc-34*	*punc-86>GFP::unc-34*
5' CTT ggA ggg TAC CgA gCT Cag AAA ATg ATT TTg CgA CAT TTC gg 3'	*cdh-3/zmp-1* extension, forward	*unc-40::GFP*	*punc-86>unc-40::GFP*
5' gTg CCA CCT gAC gTC TAA g 3'	reverse	*unc-40::GFP*	*punc-86>unc-40::GFP*
5' gTA Cgg CCg ACT AgT Agg AAA CAg T 3'	reverse nested	*unc-40::GFP*	*punc-86>unc-40::GFP*
5' CTT ggA ggg TAC CgA gCT CAg AAA ATg gTC TCA AAG ggT gAA g 3'	*cdh-3/zmp-1* extension, forward	*mCherry::moeABD*	pJWZ6
5' CAg gAA ACA gCT ATg ACC ATg 3'	reverse	*mCherry::moeABD*	pJWZ6
5' gCC gCT CTA gAA TCA TCg TTC 3'	reverse nested	*mCherry::moeABD*	pJWZ6
5'CTT ggA ggg TAC CgA gCT CAg AAA ATg gCT CAA ACA AAg CCg ATT gCC 3'	*cdh-3/zmp-1* extension, forward	*mCherry::PLCδ^{PH}*	pAA173
5' TTC gAg CgA Agg TCg CTT TTT ggT C 3'	reverse	*mCherry::PLCδ^{PH}*	pAA173
5' TTg AAA TCg AgT TgC AAg CgC gCT CC 3'	reverse nested	*mCherry::PLCδ^{PH}*	pAA173
5'CTT ggA ggg TAC CgA gCT Cag AAA Atg gCT CAA ACA AAg CCg ATT gCC 3'	*cdh-3/zmp-1* extension, forward	*mCherry*	pAA64
5' TTC gAg CgA Agg TCg CTT TTT ggT C 3'	reverse	*mCherry*	pAA64
5' TTg AAA TCg AgT TgC AAg CgC gCT CC 3'	reverse nested	*mCherry*	pAA64
5' gCA CCT CTg CTA TAT AAg AgA gTg gAA Tgg CTC AAA CAA AgC CgA TTg CC 3'	*fos-1a* extension, forward	*mCherry::PLCδ^{PH}*	pAA173
5' TTC gAg CgA Agg TCg CTT TTT ggT C 3'	reverse	*mCherry::PLCδ^{PH}*	pAA173
5' TTg AAA TCg AgT TgC AAg CgC gCT CC 3'	reverse nested	*mCherry::PLCδ^{PH}*	pAA173
5' TgT AAA ACg ACg gCC AgT 3'	forward	*unc-6>* promoter	*pVns-unc-6*
5' TgT AAA ACg ACg gCC AgT 3'	forward nested	*unc-6>* promoter	*pVns-unc-6*
5' gTT CTT CTC CTT TAC TgT TTg TgT gAA Agg gTg Taa AgT ggA3'	reverse	*unc-6>* promoter	*pVns-unc-6*
5' TCC ACT TTA CAC CCT TTC ACA CAA ACA TgA gTA AAg gAg AAg gAg AAg AACTTT TCA CTg g 3'	*unc-6* promoter extension, forward	*venus::unc-6(ΔSP)*	*pVns-unc-6*
5' CAg gAA ACA gCT ATg ACC ATg 3'	reverse	*venus::unc-6(ΔSP)*	*pVns-unc-6*
5' ATg ACC ATg ATT ACg CCA AgC gC 3'	reverse nested	*venus::unc-6(ΔSP)*	*pVns-unc-6*

(Sherwood)

Table S5. Extrachromosomal array and integrated strain generation

Ex Designation	*Is* Designation	PCR Fusion created	Injected Concentration	Co-Injection Marker(s)
qyEx27	*qyIs23, qyIs24, qyIs25*	*cdh-3>mCherry::PLCδ^{PH}*	0.01ng/µl	*unc-119*
qyEx39	*qyIs50*	*cdh-3>mCherry::moeABD*	2ng/µl	*unc-119*
qyEx40	*qyIs66, qyIs67*	*cdh-3>unc-40::GFP*	2ng/µl	*unc-119 + myo-2>YFP*
qyEx30	*qyIs37*	*zmp-1>unc-40::GFP*	2ng/µl	*unc-119*
qyEx42	*qyIs61*	*cdh-3>unc-34::GFP*	1ng/µl	*unc-119*
qyEx60	not integrated	*fos-1a>mCherry::PLCδ^{PH}*	0.25ng/µl	*pha-1*
qyEx68	*qyIs7*	*zmp-1>mCherry*	1.0ng/µl	*unc-119*
qyEx3	*qyIs17*	pGK41(*lam-1::GFP*)	10ng/µl	*unc-119*
qyEx19	*qyIs27*	pPR80(*GFP::ced-10*)	75ng/µl	*unc-119*
qyEx78	not integrated	*Venus::unc-6(ΔSP)*	15ng/µl	*unc-119*